

Modelling And Simulation of Hydrogen Production Plant for Minimum Carbon Dioxide Emission

Article Info:

Article history: Received 2023-01-07 / Accepted 2023-02-15 / Available online 2023-02-15

doi: 10.18540/jcecv19iss1pp15394-01e



Folake B. Olanrewaju

ORCID: <https://orcid.org/000000027459525X>

Department of Chemical and Petroleum Engineering, University of Uyo, Uyo, Nigeria

E-mail: folake.b.olanrewaju@gmail.com

Innocent O. Oboh

ORCID: <https://orcid.org/0000000185055729>

Department of Chemical and Petroleum Engineering, University of Uyo, Uyo, Nigeria

E-mail: innocentoboh@uniuyo.edu.ng

Olusola A. Adesina

ORCID: <https://orcid.org/0000000202173293>

Department of Chemical and Petroleum Engineering, Afe Babalola University

E-mail: adesinao@abuad.edu.ng

Chidebe Stanley Anyanwu

ORCID: <https://orcid.org/0000-0002-6059-9495>

Department of Civil and Mechanical Engineering Purdue University IN, USA

E-mail: anyacs01@pfw.edu, chidebe112@gmail.com

Daniel Raphael Ejike Ewim

ORCID: <https://orcid.org/0000-0002-7229-8980>

Department of Mechanical Engineering Durban University of Technology South Africa

E-mail: daniel.ewim@yahoo.com

Abstract

The use of coal as a source of energy for hydrogen production is desirable because it is widely available, inexpensive, and guarantees long-term availability compared to natural gas. In this study, modeling and simulation of a hydrogen production plant from coal gasification was carried out. The study also optimized process variables affecting hydrogen production for minimum carbon dioxide emissions. Modeling and simulation of a hydrogen plant was carried out using ASPEN One Suites Ver. 11 software, while optimization of process variables was done using response surface methodology (RSM). Central Composite Design (CCD) was used to design the process variables such as carbon ratio (0.715-0.75), gasification temperature (1023.15 –1223.15 K), and pressure (1-3 MPa). The independent variables for hydrogen generation and carbon dioxide emissions (CO₂e-) were correlated using a quadratic model. The coal gasification parameters were optimized numerically using the desirability function to maximize the hydrogen produced and minimize the CO₂e-. The results reveal that gasification temperature has a greater effect on maximizing hydrogen production and carbon dioxide emission (CO₂e-) reduction. Results also showed the optimal conditions for minimizing the cost and maximizing the hydrogen production: a gasification temperature of 1223.15 K, an oxygen to coal ratio of 0.715, and a gasification pressure of 1 MPa.

Keywords: Hydrogen production, optimization, ASPEN, gasification, RSM, coal energy.

1. Introduction

Different process technologies, such as natural gas reforming, processing of renewable liquid and bio-oil, biomass, and coal gasification, can be used to produce hydrogen. Also, through water splitting using a variety of energy resources and splitting of water using sunlight through biological and electrochemical materials (Hanley, Deane, and Gallachóir, 2018; Navarro, Sánchez-Sánchez, Alvarez-Galvan, Del Valle, F., and Fierro, 2010), The major drawback of using coal as a source of energy for hydrogen production is that it emits more carbon dioxide (CO₂) than other fossil fuels. The CO₂ is emitted through the coal gasification process and through water gas shift (the reaction between carbon monoxide and water to produce more hydrogen). However, hydrogen produced from coal through coal gasification technology is considered a promising opportunity due to widely available and inexpensive coal resources (Milbrandt and Mann, 2009; Minchener, 2013). Coal gasification technology is a multiphase reaction technology that involves: pyrolysis or devolatilization, coal gasification, gas clean-up or heat recovery, water gas shift reaction, and hydrogen separation (Xu *et al.*, 2014; Jeong *et al.*, 2019; and Zhang *et al.*, 2020).

As coal enters a gasifier during the pyrolysis or devolatilization process, the gasifier's hot gases dry the coal out. At temperatures below 350 °C, a number of intricate physical and chemical reactions begin gradually and quicken as the temperature rises above 700 °C. The temperature, pressure, and gas composition during pyrolysis all affect the makeup of the released products. Light gases (CO, CO₂, H₂, H₂O, and CH₄); tar, a viscous liquid made up of heavy inorganic and organic molecules; and char, a solid residue primarily made up of carbon, are the byproducts of pyrolysis. The second phase (coal gasification) is the partial oxidation of coal with oxygen and steam in a high temperature and elevated pressure process.

The process creates a synthesis gas (a mixture of predominantly carbon monoxide (CO) and hydrogen gas). The next step is the gas clean-up and heat recovery section. This step entails a number of steps: a partial quench, which dramatically lowers the gas's temperature from around 1200 °C to a fixed temperature of 800 °C, enabling the practical introduction of a series of heat exchangers that produce steam of varying quality for a dedicated steam cycle (formed by a steam turbine, condenser, and pumps), which contributes to the process's net power generation and lowers the gas's temperature to approximately 250 °C; and a hibernation cycle. After the clean-up and heat recovery section from the synthesis gas, the carbon monoxide in the gaseous mixture is reacted with more steam through the water-gas shift (WGS) reaction to produce additional hydrogen and carbon dioxide. Many studies on the optimization of coal gasification have reported the effects of variables on hydrogen production and CO₂ emissions (CO_{2e}-). Studies by Kim *et al.* (2001) and Zhou (2005) revealed that the volume % of H₂ rose with an increase in coal feed rate from 5.0 to 9.3 kg/h. While CO and CO₂ concentrations declined as a result of the decline in the O₂/coal ratio, this was caused by an increase in the supply of volatile matter. Gasification temperature plays a crucial role in carbon conversion and char gasification (Xiao *et al.*, 2006; Liu *et al.*, 2008; and Kim *et al.*, 2011). As the bed temperature increases, the carbon conversion during the gasification reaction increases by oxidation (Kim *et al.*, 2011). The present study focuses on the modeling of hydrogen production plants using coal gasification. The work also optimized the process variables for minimum carbon dioxide emissions from the plant.

Response surface methodology (RSM) was initially developed by Box and Wilson in 1951 to support the improvement of manufacturing processes in the chemical industry. It is a widely used mathematical and statistical method for modeling and analyzing a process in which the response of interest is affected by various parameters (Refinery and Braimah, 2016; Hill and Hunter, 2015). The objective of this method is to optimize the response (Montgomery, 2005). The parameters that affect the process are independent (input) variables, and the dependent (output) variables are the responses (Koç and Kaymak-Ertekin, 2009). The RSM investigates an appropriate approximation relationship between input and output variables and identifies the optimal operating parameters for a system under study or a region of the factor field that satisfies the operating requirements (Farooq *et al.*, 2013; Pishgar-Komleh *et al.*, 2012). Box-Behnken designs (BBD), central composite designs (CCD), central composite rotatable designs (CCRD), and face central composite designs (FCCD)

are experimental designs used in RSM (Wang *et al.*, 2008; Koç and Kaymak-Ertekin, 2009). A statistical methodology used for general problem solving, enhancing or optimizing product designs, and streamlining manufacturing processes is the design of experiments (DoE), a part of RSM. It seeks to choose the best areas where the reaction should be carefully investigated. Determining the accuracy of the response surface architecture is thus greatly influenced by the choice of experiment design. The benefits of the RSM can be summed up as figuring out how the independent variables interact, mathematically modeling the system, and spending less time and money by running fewer trials (Boyaci, 2005).

2. Materials and Methods

Aspen One Suites Ver. 11 software was used to simulate a coal gasification plant for hydrogen production and a pressure swing adsorption plant for oxygen production. The Design Expert Ver. 11 software was used for the optimization of the operating parameters of the coal gasification process.

2.1. Process Routes for Pressure Swing Adsorption (PSA) Plant Simulation

Table 1 indicates the feedstock properties of air used in the simulation of a pressure swing adsorption plant. The Peng-Robinson equation of state (PREoS) as shown in Equations 1–5, was used as the equation of state to calculate the streams' physical and transport properties. Figure 1 shows the flowsheet of the pressure swing adsorption simulation. A saturated air stream is created by adding water vapor (WATERVAP) to the inlet air (stream AIR-A) at a specific flow rate (SATAIR). Based on relative humidity, the temperature of saturation drums (BSATAIR) is modified. The saturated air (stream AIR-B) entered a coolant drum that reduced its temperature and was then compressed by four compression stages. The compressed air is introduced into the temperature swing adsorption (TSA) system, which separates water from compressed air. The cool, dry compressed air is separated into AIR-1 and AIR-2. The AIR-1 stream enters the high-pressure distillation column (HIGH-P) that separates the stream into nitrogen and other components. The two streams from HIGH-P and the AIR-2 stream entered the low-pressure distillation column (LOW-P) after being compressed. The LOW-P separated the entering streams into O₂ and N₂ gases. The compressors GOXCMP1, GOXCMP2, and GOXCMP3 compress O₂ before it is sent to a gasifier unit. The compressors N2CMP1, N2CMP2, and N2CMP3 also compress N₂.

Table 1 - Feedstock properties for PSA

Stream name	Air A
Stream class	CONVEN
Temperature (K)	305.372
Pressure (MPa)	0.101324
Total flowrate (kgmol/h)	16495.20
Mole fraction	
N ₂	0.781130
O ₂	0.209560
Ar	0.009310

Source: Kotz and Treichel (2011); Austin (1984); Theunis (2003).

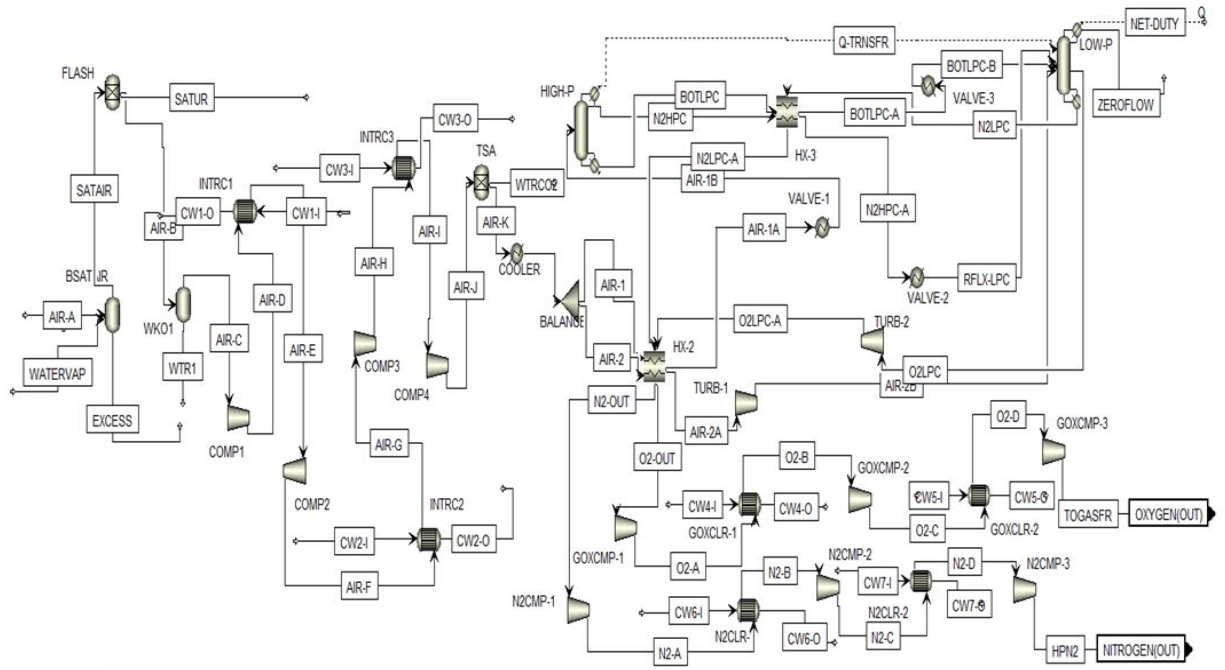


Figure 1 - Pressure swing adsorption flowsheet

The Peng-Robinson equation of State (PR EoS) are given in Eqs 1-5 as:

$$P = \frac{RT}{V_m - b} - \frac{a\alpha}{V_m^2 + 2bV_m - b^2} \quad (1)$$

$$a = \frac{0.45724R^2T_c^2}{P_c} \quad (2)$$

$$b = \frac{0.0778RT_c}{P_c} \quad (3)$$

$$\alpha = (1 + (0.37464 + 1.54226\omega - 0.2699\omega^2)(1 - T_r^{0.5}))^2 \quad (4)$$

$$T_r = \frac{T}{T_c} \quad (5)$$

Where

P , absolute pressure

R , the ideal gas constant $\approx 8.3144621 \text{ J/mol}\cdot\text{K}$

T , absolute temperature

V_m , molar volume

ω , the acentric factor for the species,

P_c , critical pressure,

T_c , critical temperature

T_r , reduced temperature

2.2. Process Routes for Gasification of Coal Plant Simulation

Coal gasification plants was simulated using coal, steam, and oxygen (produced using the pressure swing adsorption air separation method) as feedstock. The simulation has four parts: coal preparation (sizing), gasification, syngas cleaning, and water-gas shift, as shown in Figure 2. The proximate analysis, ultimate analysis, and sulfanate analysis of the coal used are as shown in Table 2.

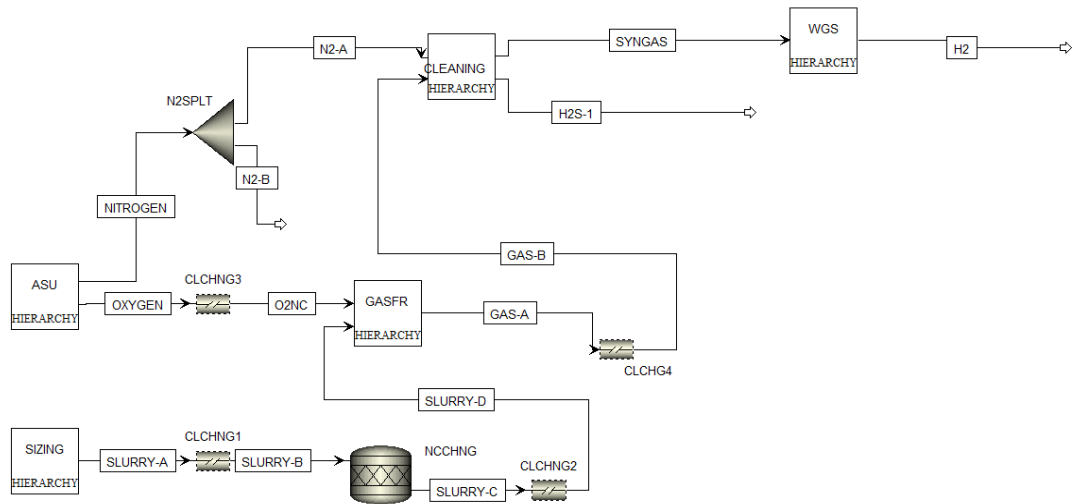


Figure 2 - The overall gasification process flowsheet

Table 2-Proximate, ultimate, and sulfanate analysis of coal used in the simulation

Characteristics	Value (%mole)
Proximate analysis	
Fixed carbon (FC)	55.44
Volatile matter (VM)	36.97
Moisture	9.07
Ash	7.59
Ultimate analysis	
Carbon	78.03
Hydrogen	5.06
Oxygen	5.66
Nitrogen	1.69
Chlorine	0.0065
Ash	7.59
Sulfanate analysis (sum is 1.97%)	
Pyritic	0.91
Sulfate	0.15
Organic	0.91

Source: Zachary (2015)

Coal preparation (sizing): Table 3 indicates the sizing hierarchy of the feedstock. The coal was mixed with water to form a slurry. The slurry was crushed with multiple roll crushers (BMILL1 and BMILL2), followed by a wet screening process that screened the slurry using a coarse split

entrainment specification as shown in Figure 3. The screened slurry entered a stoichiometric reactor as shown in Figure 2. The fractional conversion of the stoichiometric reactor is 1.

Table 3 - Feedstock properties for coal preparation.

Stream name	SL-Water	Coal
Stream class	MIXNCPSD	MIXNCPSD
Temperature (K)	332.15	288.15
Pressure (MPa)	0.101324	0.101324
Total mass flowrate (kg/h)	52616.71	142084.63

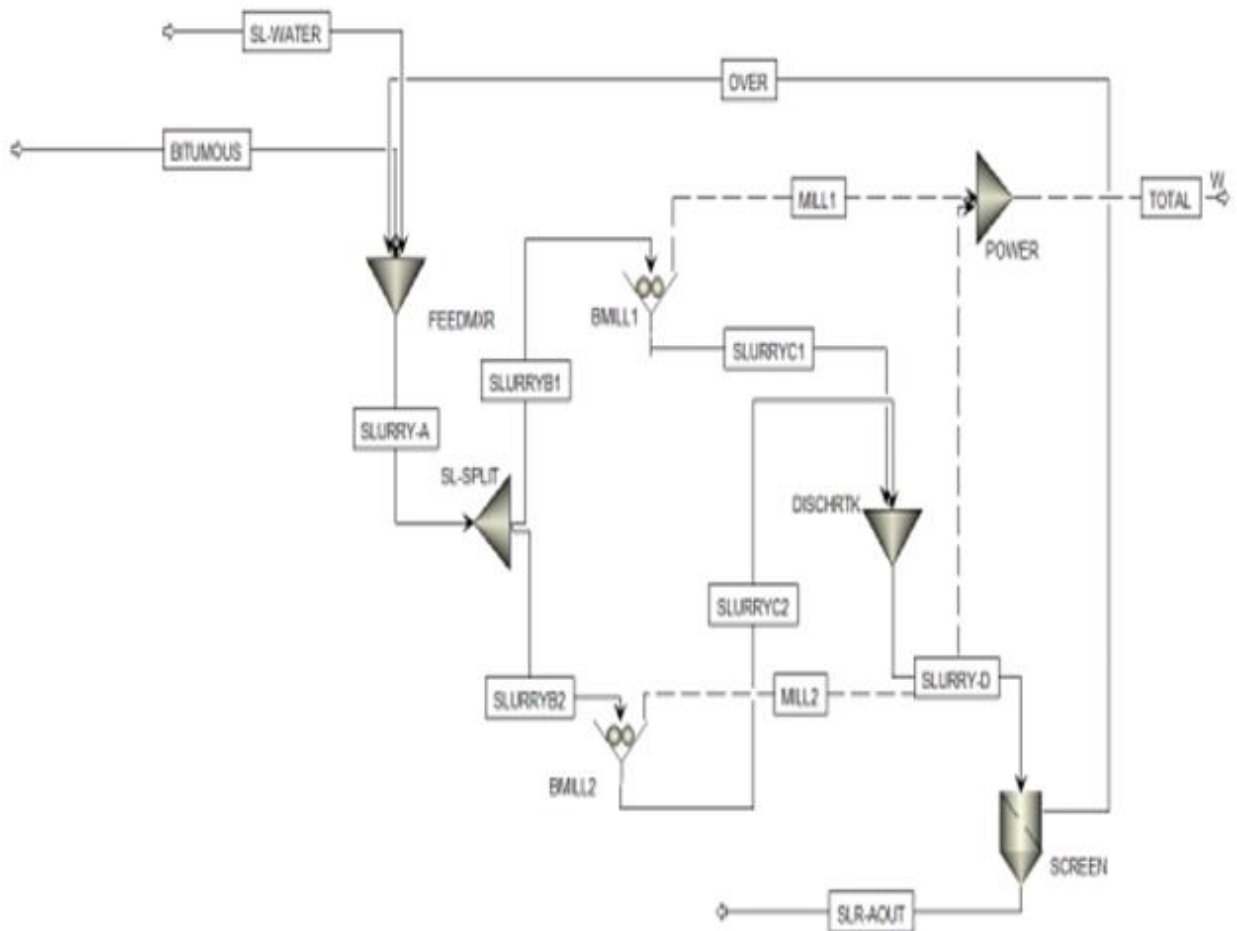


Figure 3 - Coal preparation (sizing) flowsheet

Gasification: Figure 4 shows how the compressed slurry from the sizing hierarchy enters the gasification unit and is mixed with oxygen from the air separation unit (ASU) to produce gasification effluents (A). The gasification effluents pass through heat exchangers before being passed through a component separator. The upper product of the component separator enters the sub-stream splitter that splits the stream into RSCSYNB1 and RSCSYNB2. RSCSYNB1 and RSCSYNB2 entered heat exchangers CSC1 and CSC2 before SCRUB2 and SCRUB1 (that reduced the water content, H₂S, methane, CO, CO₂, and COS). The scrubbed products (SCRBYN1 and SCRBYN2) entered COOLMX and came out as SYNGAS. The syngas passes through COSHYDR (which removes excess water) and exits as GASA(OUT).

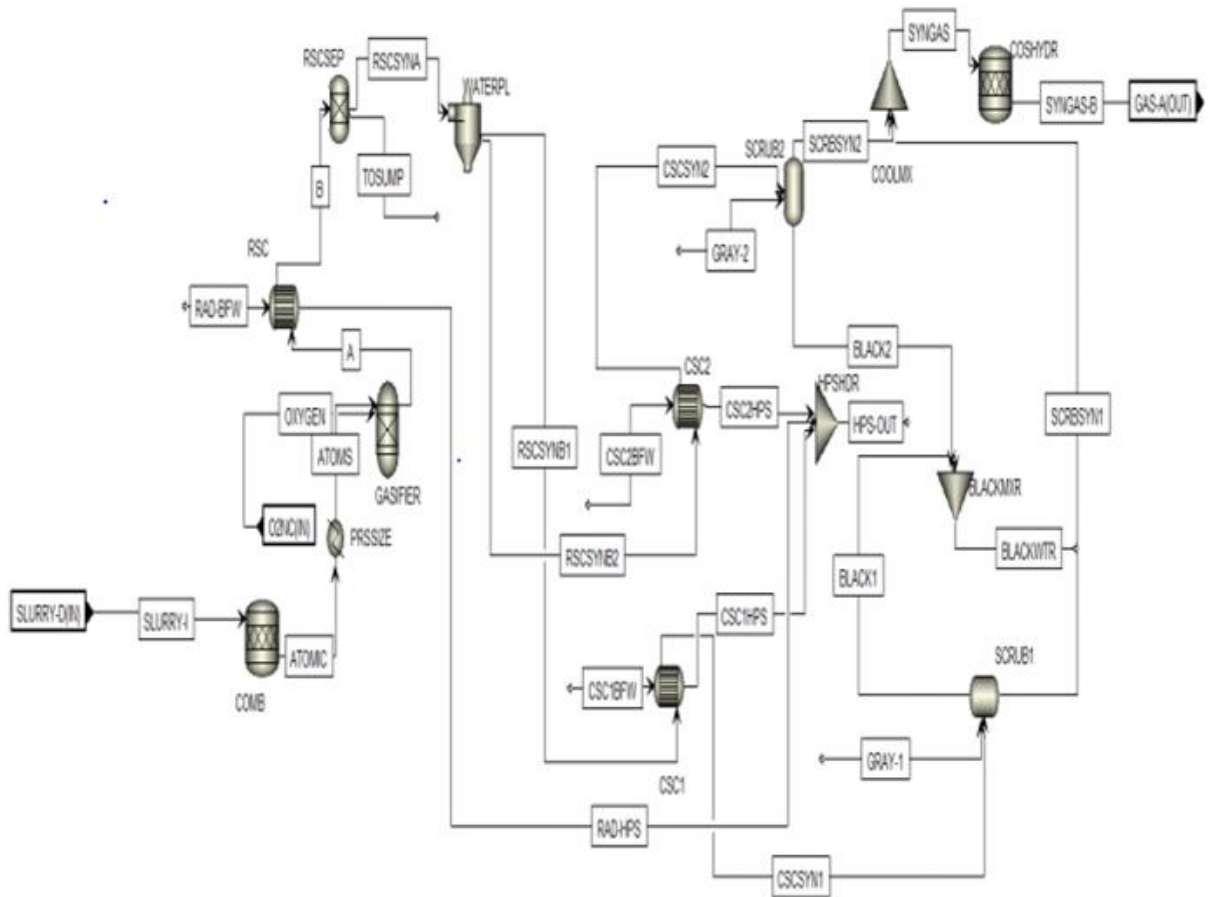


Figure 4 - Gasification flowsheet

Syngas Cleaning Unit: The cooled gas entered KODRUM for oxygen, argon, carbon monoxide, nitrogen, COS, hydrogen sulfide removal, and cleaning. The outlet gas (GAS-BB) mixed with RECYC1 and entered a 20-stage H₂S absorber to remove H₂S, producing NOH₂S and RICH-1 as shown in Figure 5. The outlet stream (NOH₂S) entered a 10-stage carbon dioxide absorber (CO₂ABS) that removes carbon dioxide, while the effluent of the CO₂ABS (TREAT) exchanged heat with stream N₂-IN to come out as TREAT-2. The H₂S absorber's other effluent gas was cooled and came out as RICH2.

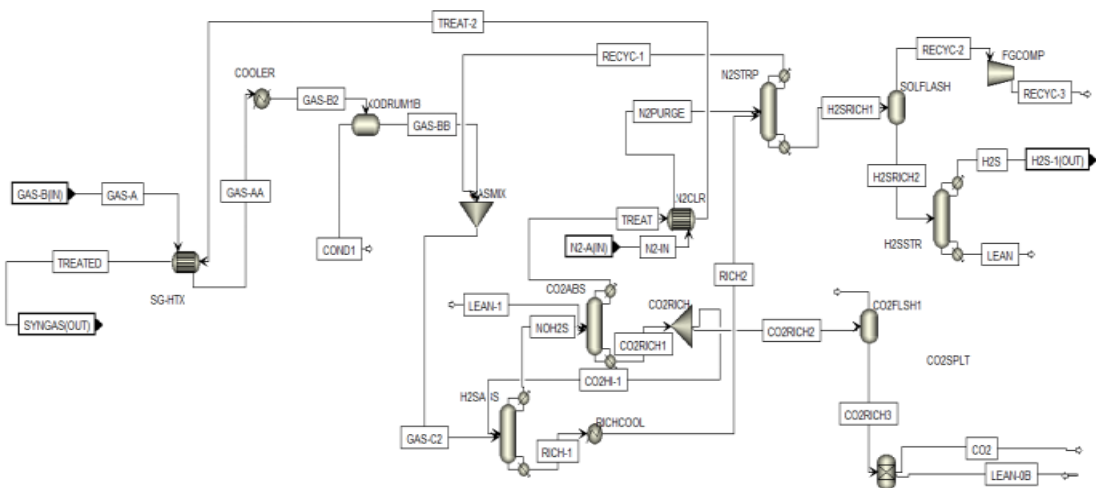


Figure 5: Syngas cleaning unit flowsheet

Using ANOVA, the probability value (p-value) at a 95% confidence interval was used to assess the model choice and model terms. Other conditions for developing a good and perfect model were also considered in the model selection. Linear, quadratic, and cubic models were tested for adequacy, but the perfect model for this study was found to be the quadratic model. The CO_{2e}- and hydrogen-production rates were investigated, and numerical optimization was performed to maximize hydrogen production while reducing CO₂.

3. Results and Discussion

3.1 Pressure Swing Adsorption

The purity of oxygen (O₂) produced is 94.4% at a mass flow of 110059.20 kg/h, as shown in Table 4.

Table 4 - Pressure swing adsorption

Parameters	Oxygen
Temperature (K)	383.50
Pressure (MPa)	4.10
Mass vapour fraction	1
Total mass flow (kg/h)	116598.75
N ₂ (kg/h)	1624.38
O ₂ (kg/h)	110059.20
Ar (kg/h)	4915.17
Purity (%)	94.40

The purity of oxygen is in good agreement with the findings of previous research. According to Santos *et al.* (2007), PSA devices are best suited for processes that do not require highly purified oxygen. Smith and Klosek (2001) performed a PSA process using zeolite to produce pure oxygen. The system was optimized based on flow, purity, and pressure, energy cost, and expected operating life and achieved an oxygen purity of typically 93–95 volume percent.

3.2. Coal Gasification Process

Table 5 shows the operating parameters CO_{2e}- and hydrogen produced from the coal gasification process. The process emitted 451,436.9 kg/h CO_{2e}- and produced 7,522.06 kg/h at a gasification temperature of 1023.15 K, an oxygen to carbon ratio of 0.75, and a pressure of 1 MPa.

Table 5 - CO_{2e}- and hydrogen produced from CG

Operating Parameters	Values
Gasification Temperature (K)	1023.15
Oxygen to carbon ratio (ratio)	0.75
Gasification pressure (MPa)	1.00
Variables	Values
CO _{2e} - (kg/h)	451436.90
Hydrogen (kg/h)	7522.06

3.3. Developing a Model

Table 6 shows the 20 experiments designed by the Design Expert software V11, together with the simulation results (responses). Design-Expert software output shows that the linear, 2FI (two factors interaction), and quadratic models were not aliased. The best-fit model proposed by the software was the quadratic versus the 2FI model.

Table 6 - Input variables in actual units and simulation (output) responses

Std	Run	Factor 1 A:Gasification Temperature (Kelvin)	Factor 2 B: Oxygen to Coal ratio (Ratio)	Factor 3 C:Gasification Pressure (MPa)	Response 1 CO ₂ e- (Kg/h)	Response 2 Hydrogen (Kg/h)
6	1	1223.15	0.715	3	189550.81	10118.9
16	2	1123.15	0.7325	2	323226.29	8814
19	3	1123.15	0.7325	2	323226.29	8814
3	4	1023.15	0.75	1	451436.90	7522.06
7	5	1023.15	0.75	3	596900.34	4852.5
1	6	1023.15	0.715	1	473935.99	7890.5
9	7	954.971	0.7325	2	637428.82	4138.6
17	8	1123.15	0.7325	2	323226.29	8814
20	9	1123.15	0.7325	2	323226.29	8814
15	10	1123.15	0.7325	2	323226.29	8814
10	11	1291.33	0.7325	2	92960.58	10441.9
13	12	1123.15	0.7325	0.318207	105580.88	11208.8
18	13	1123.15	0.7325	2	323226.29	8814
8	14	1223.15	0.75	3	173114.89	9459.2
12	15	1123.15	0.761931	2	297263.57	8417.4
2	16	1223.15	0.715	1	97741.44	11152.8
11	17	1123.15	0.703069	2	352500.24	9230.4
14	18	1123.15	0.7325	3.68179	481569.95	7139
5	19	1023.15	0.715	3	627649.37	5088.2
4	20	1223.15	0.75	1	96641.03	10314.2

The empirical relationship between response variables (CO₂e- and hydrogen yield) and the independent variables (gasification temperature, oxygen to coal ratio, and gasification pressure) are Equations 7 and 8.

$$\text{CO}_2\text{e-} = +3.237\text{e}+05 - 1.989\text{e}+5\text{A} - 11985.14\text{B} + 58261.82\text{C} + 4464.02\text{AB} - 16361.52\text{AC} - 7091.15\text{A}^2 + 21451.3\text{C}^2 \quad (7)$$

$$\text{Hydrogen} = +8814.92 + 1925.23\text{A} - 254.06\text{B} - 940.06\text{C} - 111.77\text{AB} + 447.88\text{AC} - 531.08\text{A}^2 \quad (8)$$

The factors of the model are represented by constant terms A, B, and C (linear terms), AB, AC, and BC (interactive terms), and A², B², and C² (quadratic terms). A, B, and C are coded terms used for gasification temperature, oxygen to coal ratio, and gasification pressure, respectively. These equations are for identifying the relative impact of the factors by comparing the factor coefficients. In Equation 7, the coefficient of C (58261.82) is much higher than the coefficient of interactive factor AB (4464.02), which shows that for the region studied, the C factor influences CO₂e- more than AB interaction. The coefficients of one factor represent the effect of that particular factor; the coefficients of more than one factor represent the effect of the interaction between those factors; and the coefficients of the squared factor represent the quadratic effect of that particular factor. The positive sign in front of the terms indicates a synergistic effect, while the negative sign indicates the antagonistic effect of the factor (Ani *et al.*, 2019). As suggested by Lilian and Charles (2008), analysis of variance was applied for estimating the significance of the model at the 5% significance level. ANOVA was used to estimate the statistical parameters (R², Adj-R², and predicted R²) of the coal gasification process. Tables 7 and 8 show the ANOVA table for the CO₂e- and hydrogen-production response surface quadratic model for the coal gasification process.

Table 7- ANOVA for CO₂e- response surface quadratic model for coal gasification process.

Source	Sum of Squares	Df	Mean square	F-value	P-value	
Model	2.209E+12	7	3.156E+11	2382.94	< 0.0001	Significant
A-Gasification temperature	1.697E+12	1	1.697E+12	12812.75	< 0.0001	
B-oxygen to coal ratio	9.535E+09	1	9.535E+09	71.99	< 0.0001	
C-Gasification Pressure	1.456E+11	1	1.456E+11	1098.94	< 0.0001	
AB	7.748E+08	1	7.748E+08	5.85	0.0361	
AC	1.041E+10	1	1.041E+10	78.59	< 0.0001	
A ²	1.833E+09	1	1.833E+09	13.84	0.0040	
C ²	1.678E+10	1	1.678E+10	126.65	< 0.0001	
Residual	1.324E+09	1	1.324E+09			
Cor total	2.211E+12	17				

Table 8 - ANOVA for hydrogen response surface quadratic model for coal gasification process.

Source	Sum of Squares	Df	Mean square	F-value	P-value	
Model	3.180E+08	6	5.301E+07	2393.17	< 0.0001	Significant
A-Gasification temperature	2.460E+08	1	2.460E+08	11107.67	< 0.0001	
B-oxygen to coal ratio	4.284E+06	1	4.284E+06	193.44	< 0.0001	
C-Gasification pressure	4.543E+07	1	4.543E+07	2050.94	< 0.0001	
AB	4.858E+05	1	4.858E+05	21.93	0.0005	
AC	7.799E+06	1	7.799E+06	352.11	< 0.0001	
A ²	1.926E+07	1	1.926E+07	869.35	< 0.0001	
Residual	2.658E+05	12	22149.43			
Cor total	3.183E+08	18				

According to Yi *et al.* (2010), a more significant matching coefficient is shown by a greater F-value and a smaller "P" value (prob. > F). If the p-value (significance probability value) is less than 0.05, a model term is considered significant. The models are significant, as shown by the F-values of 2382.94 and 2393.17 for the CO₂e- and hydrogen-responses, respectively. Additionally, the CO₂e-model terms (A, B, C, AB, AC, A², C²) and hydrogen-model terms (A, B, C, AB, AC, A²) in Tables 7 and 8 have P values that are less than 0.05, indicating that they are significant model terms. Additional meaningless model terms are eliminated (BC and B², as in the case of CO₂e-). Eliminating irrelevant terms makes the correlation easier to understand without compromising its accuracy. The model's statistical parameters can also be used to evaluate the model's fit quality. When the coefficient of determination (R²), which measures the percentage of the dependent variable's variation that can be predicted from the independent variable or variables, is closer to 1, the difference between the adjusted R² and the predicted R² is less than 0.2, and the adequate precision is higher than 4, a model is said to be fit. Adjusted R² not only accounts for the number of terms in a model but also shows how well terms fit a curve or line. The number of independent factors used to predict the target variable is taken into account by the adjusted R². We may next assess if the model's fit is indeed improved by including new variables. The adjusted r-squared will drop when unneeded variables are added to a model. The adjusted R-squared will rise with the addition of more beneficial variables. Adjusted R² will never be greater than R² or the same as it. The expected R² shows how accurately a regression model forecasts how fresh observations will behave. Although it is less capable of making reliable predictions for brand-new observations, it aids in determining when the model fits the original data. Predicted R² has the important advantage of preventing overfitting a model. An overfit model starts to model random noise because it has too many predictions. Random noise cannot be foreseen, hence an overfit model's expected R² must

decrease. There are almost probably too many terms in the model if the anticipated R^2 is considerably lower than the actual R-squared.

Table 9 - Statistical parameters from ANOVA for the models for CO₂e- and hydrogen of a coal gasification process

Responses	CO ₂ e-	Hydrogen
R ²	0.9994	0.9992
Adjusted R ²	0.9990	0.9987
Predicted R ²	0.9959	0.9962
Adequate Precision	157.6124	170.6436

The coefficients of determination for CO₂e- ($R^2 = 0.9994$) and hydrogen ($R^2 = 0.9992$) as shown in Table 9 were high and very close to 1; the adjusted R² values (0.9990 and 0.9987) for the CO₂e- and hydrogen responses are in reasonable agreement with their predicted R² values (0.9959 and 0.9962), that is, their difference is less than 0.2. The adequate precision that measures the signal-to-noise ratio is greater than 4 for CO₂e- and hydrogen (157.6124 and 170.6436). All of these validations showed that the simulated data for CO₂e- and hydrogen production from the coal gasification process matched the model's projected value accurately.

3.4 Interaction Effects of Input Parameters

A three-dimensional plot (3D plot) and contour plot estimated the effects of the combination of independent variables (gasification temperature, oxygen to coal ratio, and gasification pressure) on the responses (CO₂e- and hydrogen yield). Figures 7, 8, and 9 depict the independent variable's combined effect on CO₂e-

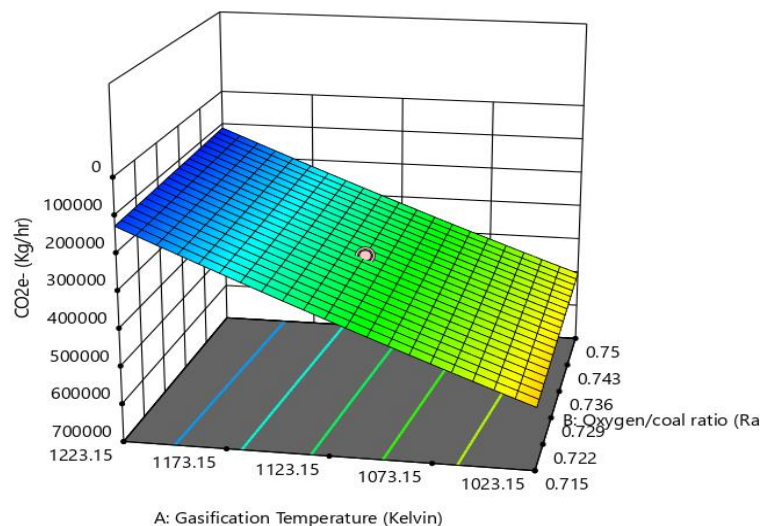


Figure 7 - Combined effect of gasification temperature and oxygen to coal ratio on CO₂e-

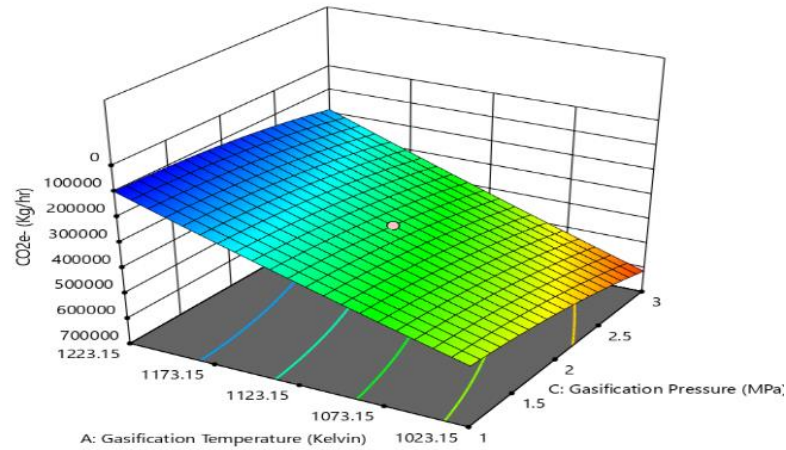


Figure 8 - Combined effect of gasification temperature and gasification pressure on CO_{2e}-

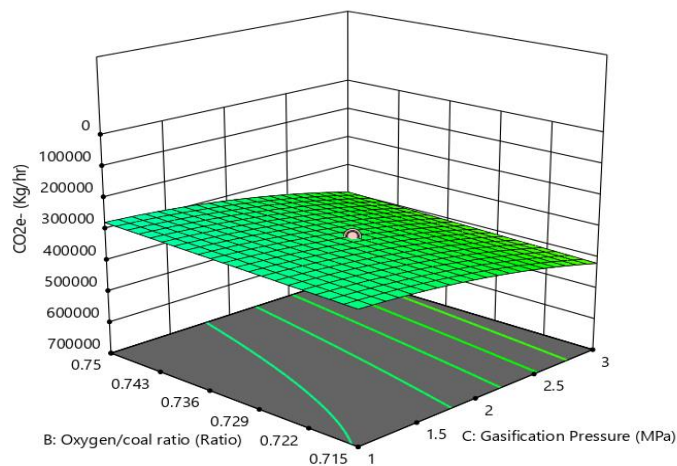


Figure 9 - Combined effect of oxygen to coal ratio and gasification pressure on CO_{2e}-

The effect of gasification temperature and oxygen-to-coal ratio on CO_{2e}- at the center level of the gasification pressure is shown in Figure 7. The CO_{2e}- decreased as the gasification temperature (A) and oxygen-to-coal ratio (B) increased at a constant gasification pressure of 2 MPa. The combined effect of gasification temperature (A) and gasification pressure (C) on CO_{2e}- at the center level of the oxygen-to-coal ratio of 0.7325 is shown in Figure 8. The results show that increasing A and decreasing C reduced CO_{2e}-. Figures 7 and 8 show a decrease in CO_{2e}- as the temperature rises. This may be due to Le Chatelier's principle (an increase in temperature favors the forward reaction of an endothermic reaction). Figure 9 indicates the effect of the oxygen-to-coal ratio (B) and gasification pressure (C) on CO_{2e}- at the center level of the gasification temperature of 1123.15 K. It can be seen from Figure 9 that CO_{2e}- increased as B decreased and C increased at a constant gasification temperature of 1123.15 K. Figures 10-12 depict the combined effect of the independent variable on hydrogen production.

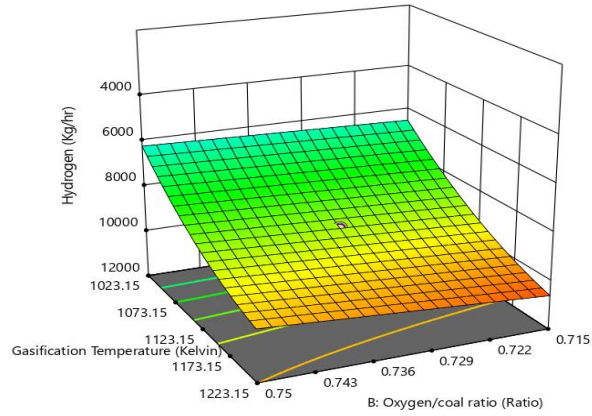


Figure 10 - Combined effect of gasification temperature and oxygen to coal ratio on hydrogen production

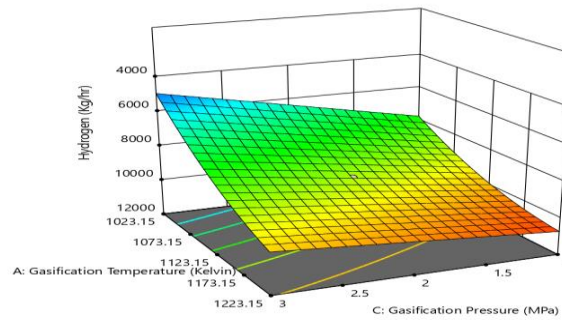


Figure 11 - Combined effect of gasification temperature and gasification pressure on hydrogen production

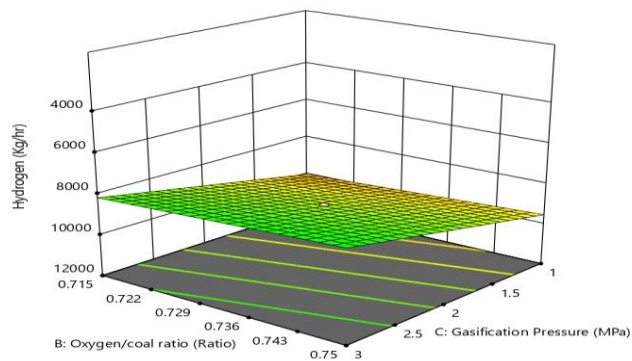


Figure 12 - Combined effect of oxygen/coal ratio and gasification pressure on hydrogen production

At the center level of gasification pressure, Figure 10 shows the impact of gasification temperature and the oxygen to carbon ratio on hydrogen yield. With a low oxygen to coal ratio and a steady gasification pressure of 2 MPa, hydrogen steadily grew as the gasification temperature increased. The high value of 1925.23 indicates that the gasification temperature has the greatest impact on the production of hydrogen, and the positive sign of coefficient A (gasification temperature) in Equation 12 demonstrates that the response grew as the gasification temperature increased. Char gasification depends heavily on the gasification temperature. The gasification reaction's conversion of carbon through oxidation to produce hydrogen and carbon dioxide increases as the bed temperature rises (Xiao *et al.*, 2006). The relationship between hydrogen yield and gasification temperature and pressure at the middle level of the oxygen-to-coal ratio is shown in Figure 11. It demonstrates that higher gasification temperatures, lower gasification pressure, and a constant oxygen to coal ratio of 0.7325 result in the production of more hydrogen. At a central temperature of 1123.15 K, Figure 8 depicts how the oxygen to carbon ratio and gasification pressure affect the creation of hydrogen. At high gasification pressure, hydrogen generation gradually declines as the oxygen content of the coal rises. It was inferred that the low hydrogen output was caused by the high oxygen to coal ratio and gasification pressure.

3.5. Numerical Optimization

Numerical optimisation in energy studies is very important (Anyanwu *et al.*, 2022). Hence, a major aspect of the study was to determine the optimum coal gasification process conditions where maximum reduction in CO₂e and hydrogen production can be obtained. Optimization of the coal gasification process variable parameter was carried out in a numerical optimization method with the Design Expert V11 to obtain optimal parameters and optimal responses. The input variables were adjusted numerically within the range goal: CO₂e was set to minimize the goal with four stars of importance, and hydrogen was set to maximize the goal with five stars of importance. The software gave 73 solutions for optimization with different desirability values ranging from 0.802 to 0.921. The ramps solution for the optimum variables (gasification temperature, oxygen to coal ratio, and gasification pressure) and corresponding responses (CO₂e and hydrogen yield) is shown in Figure 13.

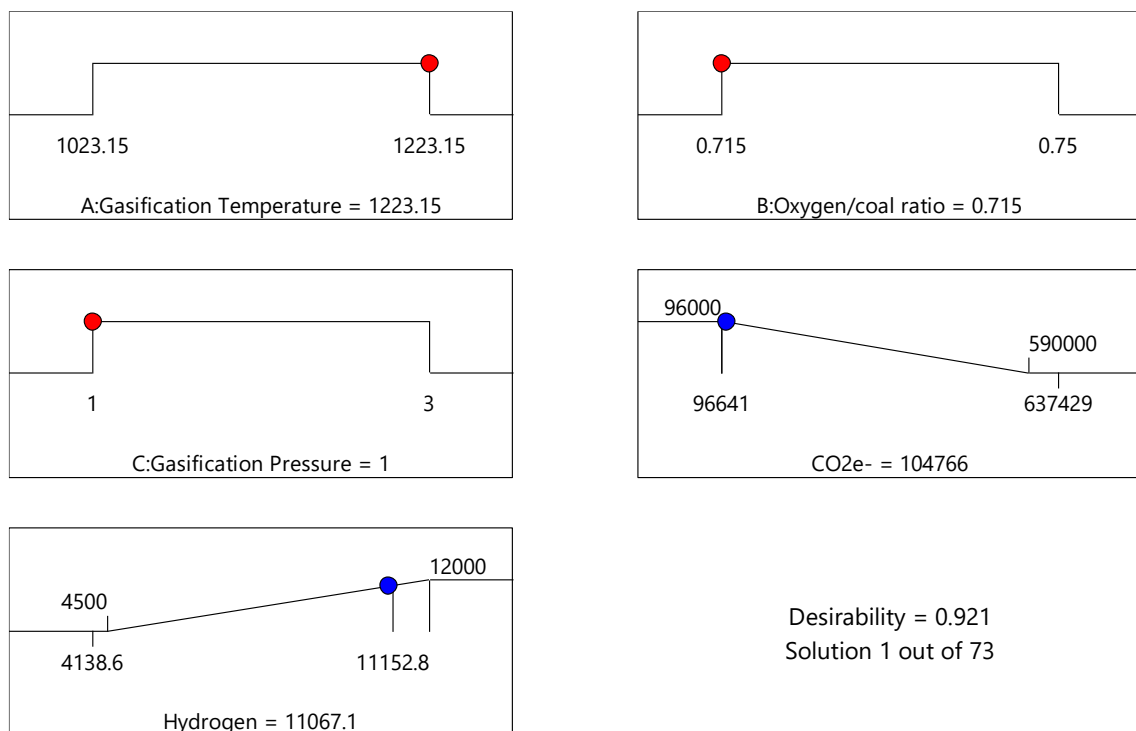


Figure 13 - Ramps of the optimum variable and their corresponding responses.

4. Conclusion

This paper simulated a pressure swing adsorption plant for oxygen production, and the oxygen produced was used as a gasification agent for coal gasification simulation for hydrogen production. The simulations were conducted using the ASPEN Plus V11 model. At optimum coal gasification process operating parameters, the extent of hydrogen generation was maximized and that of CO₂e- was minimized using the creation of an experiment tool based on response surface methodology (RSM), which is more accurate than the one-factor-at-a-time approach. The effects of three operating parameters, namely, gasification temperature, oxygen to coal ratio, and gasification pressure, and their interactions on hydrogen production and CO₂e- were studied. Design Expert V11 was used for predicting the responses in the simulation region. Using the simulation values attained at various operating conditions, regression analysis, response surface analysis, and statistical significance were performed. It was found that the gasification temperature had the greatest effect on coal's ability to produce hydrogen. Also, CO₂e- decreases as the temperature rises. This may be due to Le Chatelier's principle (an increase in temperature favors the forward reaction of an endothermic reaction). Optimal conditions for minimizing the CO₂e- from 451436.9 kg/h to 104766.422 kg/h and maximizing the hydrogen production from 7522.06 kg/h to 11067.1 kg/h were a gasification temperature of 1223.15 K, an oxygen to coal ratio of 0.715, and a gasification pressure of 1 MPa.

References

- Ani, J. U; Okoro, U. C., Aneke, L. E., Onukwuli, O. D., Obi, I. O., Akpomie, K. G. and Ofomatah, A. C. (2019). Application of response surface methodology for optimization of dissolved solids adsorption by activated coal. *Applied Water Science* 9, 60 (2019).
- Anyanwu, C. S., Gad, A., Bilal, H., & Ewim, D. R. E. (2022). Heat Analysis of a Vacuum Flask. *The Journal of Engineering and Exact Sciences*, 8(11), 15174-01e.
- Austin, G. T. (1984). *Sherve's Chemical Industries*. 5th Edition, McGraw Hill Inc., Singapore, 85p.
- Aydar, A.Y., Bağdatlıoğlu, N., Köseoğlu, O. (2017). Effect of ultrasound on olive oil extraction and optimization of ultrasound-assisted extraction of extra virgin olive oil by response surface methodology (RSM). *Grasas Y Aceites, International journal of fats and oils*. p68.
- Boyacı, İ. H. (2005). A new approach for determination of enzyme kinetic constants using response surface methodology. *Biochemical Engineering Journal*. 25:55-62.
- Bezerra, M. A., Santelli, R. E., Oliveira, E. P., Villar, L. S. and Escalera, L. A. (2008). Response surface methodology (RSM) as a tool for optimization in analytical chemistry. *Talanta-Journal*, 76: 965-977.
- Farooq, Z., Rehman, S. and Abid, M. (2013). Application of response surface methodology to optimize composite flour for the production and enhanced storability of leavened flat bread. *Journal of Food Processing and Preservation*, 37: 939-945.
- Hanley, E. S., Deane, J. P. and Gallachóir, B. P. Ó. (2018). The Role of Hydrogen in low Carbon Energy Futures- A review of existing perspectives. *Journal of Renewable and Sustainable Energy Reviews*, 82(P3): 3027-3045.
- Hill, W. J. and Hunter, W. G. (2015). Review of response surface methodology: A literature survey. *Technometrics*, 8: 571-590.
- Jeong, Y. S, Choi, Y.-K., Park, K.B. and Kim, J.-S. (2019). Air co-gasification of coal and dried sewage sludge in a two-stage gasifier: Effect of blending ratio on the producer gas composition and tar removal. *Energy* 2019, vol. 185, pp708–716.
- Kim, Y. J, Lee, S. H, Kim, S. D. (2001). Coal gasification characteristics in a downer reactor. *Fuel* vol. 80: pp1915 - 1922.
- Kim, Y.T; Seo, D. K; Hwang, J. (2011). Study of the effect of coal type and particle size on char CO₂ gasification via gas analysis. *Energy Fuels* 25:5044–5054.
- Koç, B. and Kaymak-Ertekin, F. (2009). Response surface methodology and food processing applications. *Gıda*, 7: 1-8.

- Kotz, J. C., Treichel, P. M., Treichel, D. and Townsend, J. (2011). *Chemistry and Chemical Reactivity*. Harcourt Brace and Company, Orlando, USA, 1408p.
- Lilian, S. K. and Charles, E. G. (2008). Analysis of variance: Is there a difference in means and what does it mean? *Journal of Surgical Research*, 144: 158-170.
- Liu, T. F., Fang, Y. T. and Wang, Y. (2008). An experimental investigation into the gasification reactivity of chars prepared at high temperatures. *Journal of Fuel*, 87: 460-466.
- Milbrandt, A. and Mann, R. (2009). *Hydrogen Resource Assessment Hydrogen Potential from Coal, Natural Gas, Nuclear, and Hydro Power*. A Report Submitted to National Renewable Energy Laboratory, 30p.
- Minchener, A. (2013). Challenges and opportunities for coal gasification in developing countries. *International Energy Agency Clean Coal Centre*, 3: 76p.
- Montgomery D. C. (2005). *Design and analysis of experiments*. 8th ed. New York: John Wiley and Sons Inc.
- Navarro, R. M., Alvarez-Galván, M. C., Villoria de la Mano, J. A., Al-Zahrani, S. M. and Fierro, J. L. G. (2010). A framework for visible-light water splitting. *Energy and Environmental Science*, 3(12): 1865-1873.
- Pishgar-Komleh, S. H., Keyhani, A., Msm, R. and Jafari, A. (2012). Application of response surface methodology for optimization of picker-husker harvesting losses in corn seed. *Iranica Journal of Energy and Environment*, 3(2): 134-142.
- Refinery, N. P. and Braimah, M. N. (2016). Utilization of response surface methodology (RSM) in the optimization of crude oil refinery. *Journal of Multidisciplinary Engineering Science and Technology*, 3: 4361-4369.
- Santos, J. C., Cruz, P., Regala, T; Magalhaes, F. D. and Mendes, A. (2007). High-pressure oxygen production by pressure swing adsorption. *Industrial and Engineering Chemistry Research*, 46(2): 591-599.
- Smith, A. R. and Klosek, J. (2001). A Review of air separation technologies and their integration with energy conversion processes. *Journal of Fuel Process Technology*, 70: 115-134.
- Theunis, J. K. (2003). *A Generic Framework for Continuous Energy Management at Cryogenic air Separation Plants*. MEng. Thesis, University of Pretoria, South Africa, 119p.
- Wang, J., Sun, B., Cao, Y., Tian, Y. and Li, X. (2008). Optimization of ultrasound-assisted extraction of phenolic compounds from wheat bran. *Journal of Food Chemistry*, 10(6): 804-810.
- Xiao, R., Zhang, M., Jin, B. and Huang, Y. (2006). High-temperature air or steam-blown gasification of coal in a pressurized spout-fluid bed. *Journal of Energy Fuels*, 20: 715-720.
- Xu, S., Ren, Y., Wang, B., Xu, Y., Chen, L., Wang, X. and Xiao, T.C. (2014). Development of a novel 2-stage entrained flow coal dry powder gasifier. *Applied Energy* 2014, vol. 113, pp318–323.
- Yi, S; Su, Y; Qi, B, Su Z, Wan Y. (2010). Application of response surface methodology and central composite rotatable design in optimization; the preparation condition of vinyltriethoxysilane modified silicalite/polydimethylsiloxane hybrid pervaporation membranes. *Separation and Purification Technology journal*; 71: 252–62.
- Zachary, H. (2015). *Simulation and Economic Evaluation of Coal Gasification with SETS Reforming Process for Power Production*. MSc. Thesis, Louisiana State University and Agricultural and Mechanical College, USA, 120p.
- Zhang, J., Wang, Z., Zhao, R. and Wu, J. (2020). Gasification of Shenhua Bituminous Coal with CO₂: Effect of Coal Particle Size on Kinetic Behaviour and Ash Fusibility. *Energies* vol. 13, 3313.
- Zhou, H. (2005). Air and steam coal partial gasification in an atmospheric fluidized bed. *Energy Fuel*; 19: 1619 - 1623.